

Document downloaded from:

<http://hdl.handle.net/10251/118943>

This paper must be cited as:

Pérez-Sánchez, M.; López Jiménez, PA.; Ramos, HM. (2018). Modified Affinity Laws in Hydraulic Machines towards the Best Efficiency Line. *Water Resources Management*. 32(3):829-844. <https://doi.org/10.1007/s11269-017-1841-0>



The final publication is available at

<http://doi.org/10.1007/s11269-017-1841-0>

Copyright Springer-Verlag

Additional Information

1 Modified Affinity Laws in Hydraulic Machines towards the Best Efficiency Line

2 Modesto Pérez-Sánchez ¹, P. Amparo López-Jiménez ^{1,*} and Helena M. Ramos ²

3 ¹ Hydraulic and Environmental Engineering Department, Universitat Politècnica de
4 València, Valencia, 46022 Spain; mopesan1@upv.es

5 ² Civil Engineering, Architecture and Georesources Department, CERIS, Instituto Superior
6 Técnico, Universidade de Lisboa, Lisboa, 1049-001, Portugal; hramos.ist@gmail.com

7 * Correspondence: palopez@upv.es; Tel.: +34-96-387700 (ext. 86106)

8

9 ABSTRACT

10 The development of hydraulic and optimization models in water networks analyses to improve
11 the sustainability and efficiency through the installation of micro or pico hydropower is
12 swelling. Hydraulic machines involved in these models have to operate with different rotational
13 speed, in order that in each instant to maximize the recovered energy. When the changes of
14 rotational speed are determined using affinity laws, the errors can be significant. Detailed
15 analyses are developed in this research through experimental tests to validate and propose new
16 affinity laws in different reaction turbomachines. Once the errors have been analyzed, a
17 methodology to modify the affinity laws is applied to radial and axial turbines. An empirical
18 method to obtain the Best Efficiency Line (BEL) in proposed (*i.e.*, based on all the Best
19 Efficiency Points (BEPs) for different flows). When the experimental measurements and the
20 calculated values by the empirical method are compared, the mean errors are reduced 81.81 %,
21 50%, and 86.67% for flow, head, and efficiency parameters, respectively. The knowledge of
22 BEL allows managers to define the operation rules to reach the BEP for each flow, improving
23 the energy efficiency in the optimization strategies to be adopted.

24 **KEYWORDS:** affinity laws, best efficiency line (BEL), variation operating strategies, energy

25 recovery

26

27 **1 Introduction**

28 Nowadays, the development of mathematical models to analyse the behavior of hydraulic
29 systems requires theoretical and experimental laws. In some cases, the direct application of
30 these equations can lead to erroneous results (Simpson and Marchi 2013), being necessary to
31 correct them in order to consider the necessary simplifications in the initial assumptions (e.g.
32 viscosity effects, friction losses, turbulence, vortex). In water distribution networks, the model
33 simulation with installed hydraulic machines is very common, and the energy analyses have a
34 great significance due to the increasing price of the energy (Corominas 2010) and the need to
35 reduce the energy consumption and the system efficiency to satisfy the European standards
36 requirements (Pasten and Santamarina 2012).

37 Traditionally, these optimizations of energy consumption in water systems have been focused
38 on the reduction of consumed power by installed pumps. Hence, some authors have worked in
39 the development of pumped systems to adapt the rotational speed of the machine to reduce the
40 energy consumption (Sarbu and Borza 1998; Moreno et al. 2010; Simpson and Marchi 2013;
41 Jiménez-Bello et al. 2015) and the pressure in the system (Kevin 1990; Giustolisi et al. 2008;
42 Cabrera et al. 2014). These reductions are of paramount importance in economic and
43 environmental savings, which have been analyzed through different algorithms and software
44 such as *EPANET* (Rossman 2000) or *WaterGEMS* (Nazari and Meisami 2008), providing
45 significant tools for water management in pipe systems.

46 In the last years, different authors have developed researches using new technologies to
47 leverage the pressure reduction in water distribution networks, increasing the global efficiency
48 in the water system (Abbott and Cohen 2009; Dannier et al. 2015; Pérez-Sánchez et al., 2017).
49 Araujo et al. (2006) and Giugni et al. (2014) enumerate different algorithms to optimize the
50 location the optimal place of the **Pressure Reduction Valves (PRVs)** in a network for leakages
51 control. The initial **study of Pump Working as Turbines (PATs) that are** installed in water

52 systems to replace *PRVs* (Ramos and Borga, 1999) allowed modellers to analyze the turbine
53 behaviour according to different aspects such as:

- 54 • The morphology of the machine (Yang et al. 2012; Carravetta et al. 2013a; Shi et al.
55 2015).
- 56 • The design of installation schemes and operation strategies (Carravetta et al. 2012,
57 2014b; Fontana et al., 2012).
- 58 • The design of machines, adapted to specific work conditions (i.e. low head and high
59 range of flows) in these water drinking network such as the tubular propeller (Ramos et
60 al. 2013; Samora et al. 2016b).
- 61 • The analysis of potential recovered energy according to circulating flow along the time
62 through of simulated annealing techniques (Pérez-Sánchez et al. 2016; Samora et al.
63 2016a; Pérez-Sánchez et al., 2018).
- 64 • The economic and feasibility analyses of these installations showing the sustainability
65 and environmental profit of these solutions (Ramos et al. 2010; McNabola et al. 2014).

66 Furthermore, the study of the performance behavior of these machines, Singh (2005) and
67 Derakhshan and Nourbakhsh (2008) proposed the efficiency and head curves as function of
68 flow according to the specific rotational speed of the machine. These curves can be used in the
69 simulations of energy analyses with good results when the hydraulic machine operates in its
70 nominal rotational speed. However, if the energy studies consider operation strategies with
71 variation of the rotational speed, the use of affinity laws in the simulations can bring erroneous
72 results of recovered energy in the system (Sarbu and Borza 1998; Gulich 2003) since the
73 turbines do not behave as the similarity described. Therefore, considering the need to know the
74 efficiency of the machine as function of rotational speed, the first aim of this research is to
75 obtain the errors between measured and calculated efficiency through the application of affinity

76 laws. This analysis was developed for two machines (with axial and radial impellers) based on
77 experimentation. The second objective is to develop modified affinity laws to establish the best
78 efficiency line (*BEL*) and the best efficiency head (*BEH*) of each machine as function of flow.
79 *BEL* and *BEH* establish the rotational speed of the machine when the Variable Operating
80 Strategies (*VOS*) are used (Carravetta et al. 2013b), claiming for each flow the best operation
81 point (*BEP*). The development of both objectives presents the main novelty of this research that
82 obtains the *BEL* and *BEH*. These lines can be used on optimization techniques to maximize the
83 recovered energy in water distribution system when the rotational speed changes, obtaining
84 result more exactly than the values when similarity laws are used.

85 2 Material and Methods

86 2.1 Type of Hydraulic machines

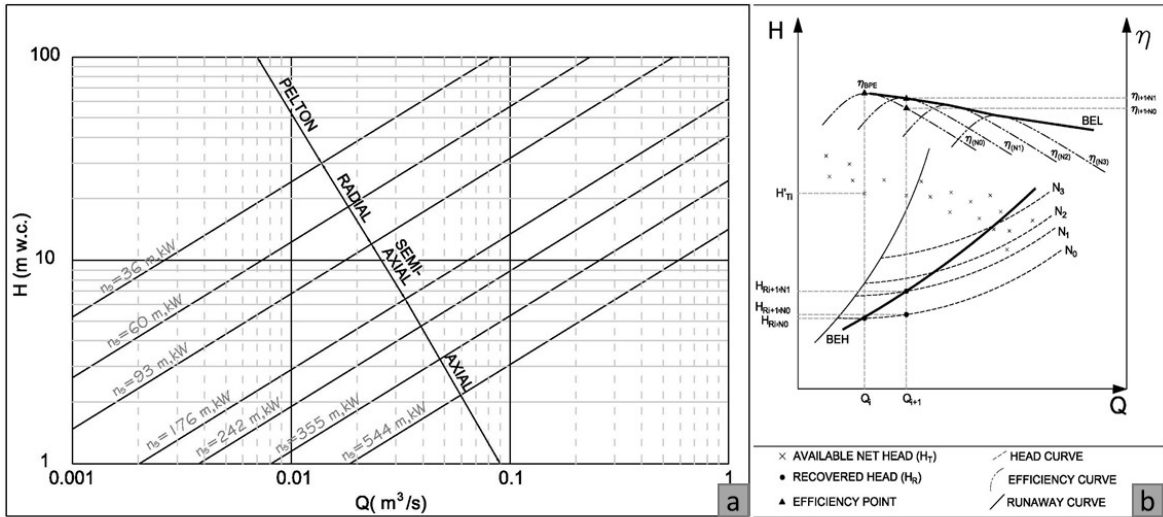
87 A general typification of hydraulic machines refers to action or reaction according to the
88 exchange of energy between fluid and impeller at atmospheric pressure or not. Inside the group
89 of the reaction machines, the impeller shape and the specific speed establish a second
90 classification. This parameter is defined as the rotational speed of a similarity turbine
91 (geometrically) to generate one kW when the head is equal to one. The specific speed
92 establishes the impellers' typology and it is defined by equation (1):

$$93 \quad n_s = n \frac{P^{1/2}}{H^{5/4}} \quad (1)$$

94 where n_s is the specific speed of the machine in (m, kW); n is the rotational speed of the
95 machine in rpm; P is the power in shaft, which is measured in (kW); and H is the recovered
96 head in (m w.c.).

97 Based on the specific speed, the impellers can be: radial, semi-axial, or axial according to Figure
98 1a. The radial or centrifugal impeller are those in which the fluid enters in the machine in radial
99 direction and exists in axial direction. This type of machines has a specific speed number

100 between 36 and 93 rpm. For n_s between 93 and 176 rpm, the machine is called diagonal or
 101 semi-axial. In this sort of machines, the inlet of the fluid is diagonal while the outlet has an axial
 102 direction. Finally, the axial machines present the fluid direction both inlet and outlet with axial
 103 direction and the specific speed is greater than 176 rpm.



104
 105 **Fig. 1 (a) Type of impeller according to specific rotational speed (adapted from Alexander et**
 106 **al. 2009) and (b) scheme of operating points**

107 **2.2 Theoretical approximation: affinity laws**

108 The study of the behavior of turbomachines with equal specific rotational speed can be tackled
 109 if the conditions of similarity (geometrical, kinematic and dynamic) are entailed. The first
 110 condition is satisfied, when the study is focused on analyzing the **behaviour** of a machine with
 111 different rotational speed. Kinematic condition establishes that in the inlet and outlet impeller,
 112 the triangles are similar. These two conditions are defined by equations (2) to (4) (Mataix,
 113 2009):

114
$$\frac{Q_1}{Q_0} = \left(\frac{D_1}{D_0}\right)^3 \frac{N_1}{N_0} \tag{2}$$

$$115 \quad \frac{H_1}{H_0} = \left(\frac{D_1}{D_0}\right)^2 \left(\frac{N_1}{N_0}\right)^2$$

$$116 \quad (3)$$

$$117 \quad \frac{P_1}{P_0} = \left(\frac{D_1}{D_0}\right)^2 \left(\frac{N_1}{N_0}\right)^3$$

$$118 \quad (4)$$

119 where Q_1 is the flow in the new conditions of rotational speed in m^3/s ; Q_0 is the flow in nominal
 120 rotational speed in m^3/s for the *BEP*; D_1 is the diameter of the impeller in new situation of
 121 rotational speed in m; D_0 is the nominal diameter of the impeller in m; N_1 is the new rotational
 122 speed in rpm; N_0 is the nominal rotational speed of the impeller in rpm; H_1 is the head in new
 123 condition in m w.c.; H_0 is the head in the nominal conditions in m w.c.; P_1 is the shaft power
 124 in new conditions in kW; and P_0 is the shaft power in the nominal condition in kW.

125 Therefore, if hydraulic parameters of the turbomachine (flow, head, and power) can be related
 126 through affinity laws and the efficiency of the machine can be indirectly determined for
 127 different rotational speeds, keeping the impeller's size. Based on this assumption, equations (2)
 128 to (4) can be simplified into equations (5) to (7) (Mataix 2009):

$$129 \quad \frac{Q_1}{Q_0} = \frac{N_1}{N_0} = \alpha \quad (5)$$

$$130 \quad \frac{H_1}{H_0} = \left(\frac{N_1}{N_0}\right)^2 = \alpha^2 \quad (6)$$

$$131 \quad \frac{P_1}{P_0} = \left(\frac{N_1}{N_0}\right)^3 = \alpha^3$$

$$132 \quad (7)$$

133 where α is the ratio between N_1 and N_0 .

134 The characteristic curve of a turbomachine (as a second-degree polynomial) can be written by
135 equation (8) (Mataix 2009):

$$136 \quad H_0 = AQ_0^2 + BQ_0 + C$$

137 (8)

138 where A , B , and C are coefficients of the characteristic curve.

139 The efficiency curve can be also established by a second (Mataix 2009) **around the nominal**
140 **point**, or by third-degree polynomial if a discretized range of flows is considered (Ulanicki et
141 al. 2008). The nominal efficiency curve is then defined by equation (9):

$$142 \quad \eta_0 = EQ_0^3 + FQ_0^2 + GQ_0 + I \quad (9)$$

143 where: η_0 is the efficiency of the machine for a flow equal to Q_0 ; E , F , G , and I are coefficients
144 of efficiency curve.

145 When the affinity laws are applied to equations (8) and (9), the new curves of the turbomachines
146 are defined by equations (10) and (11):

$$147 \quad H_1 = AQ_1^2 + \alpha Q_1 + \alpha^2 C$$

148 (10)

$$149 \quad \eta_1 = \frac{E}{\alpha^3} Q_1^3 + \frac{F}{\alpha^2} Q_1^2 + \frac{G}{\alpha} Q_1 + I$$

150 (11)

151 where: η_1 is the efficiency of the turbine for a flow equal to Q_1 .

152 **2.3 Experimental approximation: efficiency curves**

153 The prediction of head and flow values in turbines working with different rotational speeds has
154 a reasonable approximation. Nevertheless, as the affinity laws do not consider the viscosity

155 effects of the fluid inside of the impeller (third condition of similarity), the use of these laws is
156 limited (Simpson and Marchi 2013). Hence, these equations cannot be applied in all flow range
157 to predict the performance, obtaining good results in turbines for ranges between +/- 20%
158 around of the best efficiency point. As the viscosity effect has to be considered, the dynamic
159 similarity is important in these cases. This effect must be **considered** together with geometrical
160 and kinematic similarity. To consider the dynamic condition, different researchers (Sarbu and
161 Borza 1998; Gulich 2003; Simpson and Marchi 2013) have proposed equations to define the
162 performance as function of the rotational speed variation. Gulich (2003) proposed the equation
163 (12), which predicts the performance according to the variation of Reynolds number between
164 both rotational speeds of the machine.

$$165 \quad \frac{1-\eta_1}{1-\eta_0} = K + (1 - K) \left(\frac{Re_1}{Re_0} \right)^2 \quad (12)$$

166 where Re_1 is the Reynolds number for the rotational speed N_1 ; Re_0 is the Reynolds number for
167 the rotational speed N_0 ; K is the loss coefficient in the impeller as function of the Reynolds
168 number.

169 Similar equation was proposed by Sarbu and Borza (1998), who also related the Reynold
170 number as function of the rotational speed, defined in equation (13):

$$171 \quad \frac{1-\eta_1}{1-\eta_0} = \left(\frac{N_1}{N_0} \right)^{0.1} \quad (13)$$

172 Equations (12) and (13) were tested by Simpson and Marchi (2013), obtaining good results in
173 the prediction of the efficiency, if the rotational speed is not reduced under to 70% of the
174 nominal speed. This is due to the empirical expression exponent changes with viscosity and
175 friction effects in the impeller.

176 When variable operating strategy (VOS) is applied, the final objective is to determine the best
 177 efficiency line (BEL) as function of the rotational speed for each flow (Figure 1b). The
 178 operation point should be fixed in the available maximum point to maximize the efficiency of
 179 the recovery system. The knowledge of *BEP* for each flow along the time (*i.e.*, Q_i , Q_{i+1}) as well
 180 as the available net head (H_{Ti}) will allow researchers to know the best efficiency head line
 181 (BEH) of the installed machine ($H_{Ri,N0}$, $H_{Ri+1,N1}$) for the recovery system. Both lines allow to
 182 recover the maximum energy, helping to define the VOS in the system for the necessary
 183 rotational speed (*i.e.*, N_0 , N_2 , ..., N_i) in each time.

184 Traditionally, these variations have been predicted by affinity laws, but only near the *BEP*. In
 185 this *BEL*, different authors (Carravetta et al. 2014a, 2014b; Fecarotta et al. 2016) proposed
 186 modifications in the affinity laws to improve the prediction of the *BEP* depending on the
 187 rotational speed. This proposal was developed for some semi-axial machines with specific
 188 rotational speed between 120 and 162 (m, kW). As proposed, the modification of the affinity
 189 laws is developed according to the equations (5) to (7) as well as the use of the Suter Parameters
 190 (*SP*), which were defined by Suter (1966) by equations (14) and (15):

191 - Head SP; $WH = \frac{h}{n^2+q^2}$ (14)

192

193 - Torque SP; $WT = \frac{b}{n^2+q^2}$ (15)

194

195 where h , q , n , and b are the head, discharge, velocity, and torque coefficients defined by
 196 equations (16) to (19), respectively.

197 - Head coefficient: $h = \frac{H}{H_0}$

198 (16)

199

200 - Discharge coefficient: $q = \frac{Q}{Q_0}$

201 (17)

202

203 - Velocity coefficient: $n = \frac{N}{N_0}$

204 (18)

205

206 - Torque coefficient: $b = \frac{T}{T_0}$ (19)

207

208 Finally, the performance coefficient (e) (which is also called efficiency ratio) is defined by
209 equation (20):

$$210 \quad e = \frac{\eta}{\eta_B} = \frac{bn}{qh} = \tan\varphi \frac{WT}{WH}$$

211 (20)

212

213 where $\tan\varphi$ is the ratio between q and n , according to the third quadrant ($p < \varphi < 3p/2$), when the
214 machine is working as turbine (*PAT*). In this case, h and b are positive, while n and q are
215 negative. According to expert references (Carravetta et al. 2014a, 2014b; Fecarotta et al. 2016),
216 the affinity laws can be modified as:

$$217 \quad q = \frac{Q_1}{Q_0} = f_1(\alpha)$$

218 (21)

$$219 \quad h = \frac{H_1}{H_0} = f_2(\alpha)$$

220 (22)

221 $p = \frac{P_1}{P_0} = f_3(\alpha)$

222 (23)

223 where f_1, f_2 , and f_3 are fitted **functions that depend** on the experimental data according to α .

224 **2.4 Theoretical vs. Experimental: error definition**

225 The determination of the errors is evaluated by equations (24) and (25). Three comparisons
226 have been done: a) experimental data versus classic affinity laws; b) experimental data versus
227 modified affinity laws; and experimental data versus empirical method. Equation (24) defines
228 the absolute relative error between the experimental data and estimated measurements for the
229 same flow value (head or efficiency) and equation (25) defines the mean square error, which is
230 determined according to the number of measured data:

231 *Absolute error* (ε_i) = $\left| \frac{X_{est} - X_{exp}}{X_{exp}} \right|$

232 (24)

233 *Mean square error* (σ_i) = $\frac{1}{m} \sqrt{\sum_{i=1}^m \left(\frac{X_{est} - X_{exp}}{X_{exp}} \right)^2}$

234 (25)

235 where i is the tested parameter, which can be q, h, p , or e ; X_{est} is the estimated value through
236 affinity laws or empirical method; X_{exp} is the measured value; and m is the number of
237 measurements.

238 **3 Developed Test**

239 **3.1 Tested Impellers**

240 The experimental tests have been carried out in CERIS-Hydraulic Lab of Instituto Superior
241 Técnico from the University of Lisbon with two different machines. In both cases the discharge

242 was measured by an electromagnetic flowmeter, the pressure was registered by pressure
243 transducers, and the power by digital wattmeter FLUKE which was connected to the generator.
244 The digital multimeter is able to measure active power, reactive power and power factor.
245 Finally, the rotational speed was measured by a frequency meter.

246 Two different machines were tested (Figure 2). On the one hand, an axial machine with an
247 impeller's size of 85 mm with five blades. This machine has the best efficiency point for a flow
248 of 4.44 l/s and head of 0.24 m w.c.. when the nominal rotational speed is 750 rpm. For this
249 machine, the specific speed number is 283 (m, kW) (Eq. (1)). On the other hand, a radial
250 machine that has an impeller size of 139 mm. For this machine, when the rotational speed is
251 1020 rpm, the best efficiency point is located for 3.36 l/s and 4 m w.c. and the specific rotational
252 speed is 51 (m, kW). The generator connected to both machines has a maximum efficiency of
253 62% when the rotational speed is 1350 rpm. The characteristics of the generator are: the rated
254 frequency 50 Hz, the rated power 550 W, the rated current 1.6/2.8 A, the rated phase voltage
255 230/400 V, the power factor 0.74 and the rated speed 1020 rpm.

256 3.2 Rotational speed variation

257 In Figures 2a and 2b, the efficiency and head curve for different rotational speed are shown
258 according to the performed tests in the axial machine. In this case, these figures show the head
259 values and the efficiency as function of the flow for different rotational speeds (500, 750, 1000,
260 1250, and 1500 rpm) as well as the runaway curve.

261 These characteristic curves for a rotational speed of 750 rpm can be fitted by polynomial
262 equations (26) and (27):

263 - Head curve (m w.c.):

$$264 \quad H = 0.047Q^2 - 0.219Q + 0.272 \quad (R^2 = 0.998) [4.40 < Q < 13.30 \text{ l/s}]$$

265 (26)

266 - Efficiency (%):

267
$$E = -0.058Q^4 + 1.942Q^3 - 23.690Q^2 + 118.381Q - 143.852 \quad (R^2=0.995). \quad [4.40 < Q$$

268
$$< 13.30 \text{ l/s}] \quad (27)$$

269 When the machine is operating in its nominal rotational speed, the flow range oscillates between
270 4.40 l/s and 13.30 l/s, varying the recovered head between 0.26 and 5.88 m w.c.. For this range
271 of flows, the efficiency of the machine oscillates between 63.65 % and 29.62%, being the
272 maximum efficiency of 63.65%, when the flow is 4.44 l/s.

273 **Figures 2c and 2d show** similar results according to tests carried out with the radial machine.

274 In this case, the machine was tested for 600, 900, 1020, and 1200 rpm. The characteristic curve
275 is presented for a rotational speed of 1020 rpm, being defined by the following equations (28)
276 and (29):

277 - Head curve (m w.c.):

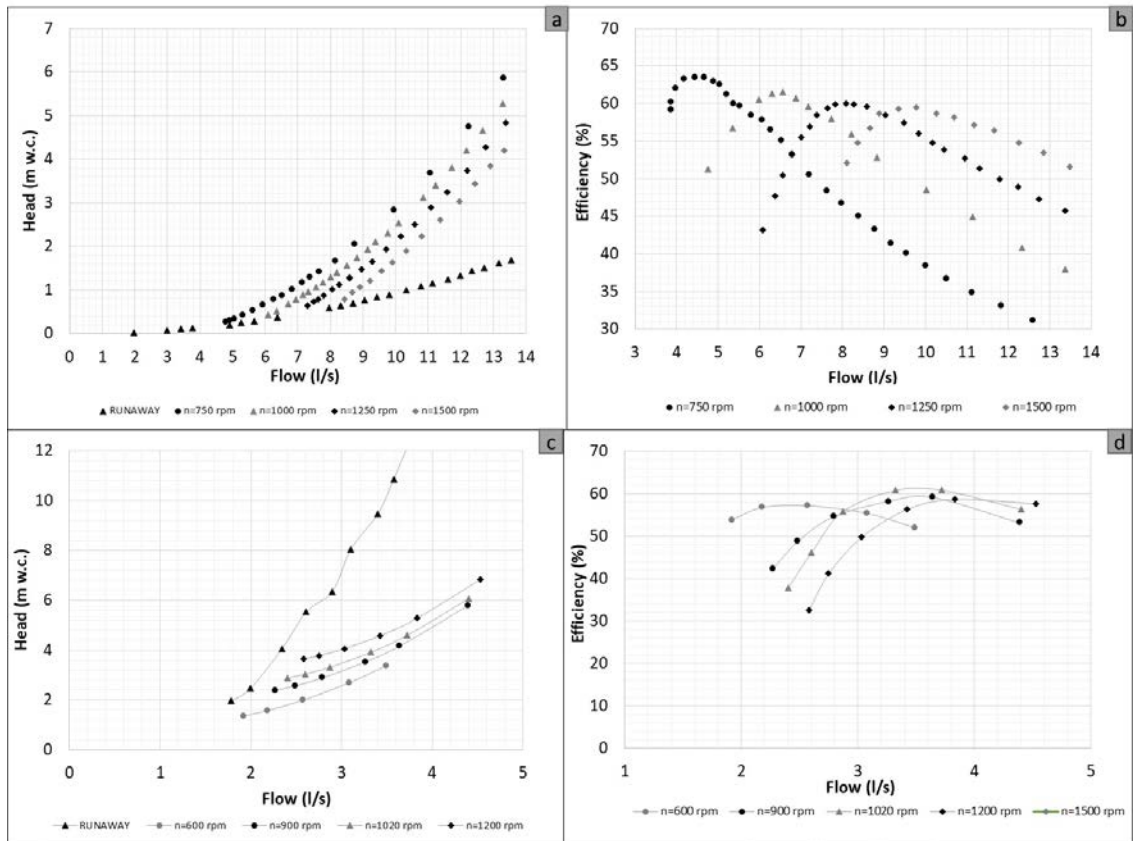
278
$$H = 0.431Q^2 - 1.310Q + 3.553 \quad (R^2 = 0.995) \quad [1.80 < Q < 4.40 \text{ l/s}]$$

279
$$(28)$$

280 - Efficiency (%):

281
$$E = -11.145Q^2 + 80.698Q - 84.535 \quad (R^2=0.995) \quad [4.80 < Q < 13.30 \text{ l/s}]$$

282
$$(29)$$



283

284 **Fig. 2** Experimental data (Head and Efficiency) for machines: (a and b: axial; c and d,
 285 radial).

286 For this machine, the maximum efficiency is 60.5% for a flow of 3.36 l/s.

287 The runaway curves are also shown in Figures 2a and 2c for both machines (axial and radial).

288 When these curves are analyzed, a significant difference can be determined taking into account
 289 the VOS. If a same value of the recovered head is established, a reduction of the flow with a
 290 high rotational speed can lead to cause the runaway condition in radial machines. In the case of
 291 the axial machine, an increasing of the flow keeping the recovered head can be attained the
 292 runaway conditions.

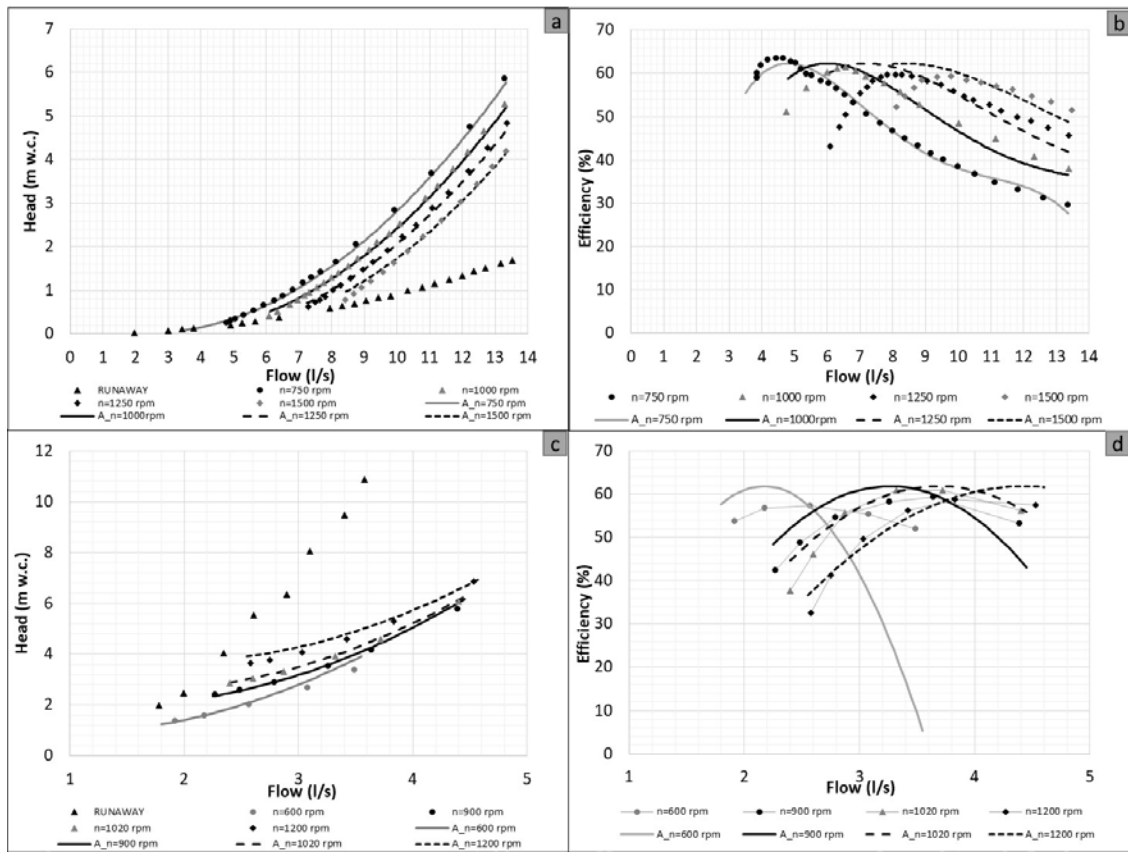
293 3.3 Analytical versus experimental curves

294 The need to know the head and efficiency values of each machine can lead to develop new
 295 curves with different rotational speeds through affinity laws or Suter parameters, when the

296 water manager uses VOS. The obtained results in analyses of axial and radial machines are
297 shown in Figure 3. The head values of the affinity laws can be observed, coinciding on a great
298 range of flow conditions. Therefore, the use of these laws to develop new equation of recovered
299 head curve can be used. Otherwise, if water managers want to determine the efficiency, the
300 affinity laws can fail. Figures 4b and 4d show the predicted efficiencies given by the affinity
301 laws, which are different, especially when the maximum values are considered (*i.e.*, maximum
302 efficiency and flow value).

303 As shown in Figures 3a and 3b, in the axial machine when the rotational speed is 750 rpm, the
304 maximum efficiency is 63.60% for a flow of 4.66 l/s, while the maximum efficiency by affinity
305 laws is 62.19%. For the rotational speed of 1000 rpm, the maximum efficiency is 61.56% when
306 the flow is 6.56 l/s, being the maximum efficiency by the affinity laws 62.27% when the flow
307 is 6.03 l/s. This error raises with rotational speeds of 1250 and 1500 rpm. For the rotational
308 speed of 1250 rpm, the maximum measured efficiency is 59.98% and the maximum estimated
309 efficiency is 62.27 %, being the flow values of 8.28 and 7.21 l/s, respectively. Similar tendency
310 can be observed in Figure 3b when the rotational speed is 1500 rpm.

311 Figures 3c and 3d show results between measured efficiencies and estimated values by affinity
312 laws for different rotational speeds of 600, 900, 1020, and 1200 rpm in the radial machine, not
313 being coincident the *BEP* for each rotational speed (*e.g.*, when the rotational speed is 900 rpm,
314 the maximum measured efficiency is 59.23% and the maximum estimated efficiency is 61.82%,
315 being the flows 3.65 l/s and 3.25 l/s, respectively).



316

317

Fig. 3 Experimental vs affinity laws in the axial (a and b) and radial machine (c and d)

318

Figure 4a shows the absolute error between experimental data and estimated values by affinity

319

laws used to predict head and efficiency for flows (Q) and rotational speeds (N) in the axial

320

machine. The majority of head errors can attain 10% in both cases (axial and radial machines).

321

If efficiency predictions errors are analyzed, the best fits are located in low value zone of

322

efficiency curve, being these errors below to 1%. Figure 4a also shows the maximum errors are

323

near the maximum efficiency point. In the case of radial machine (Figure 4b), this trend does

324

not occur as for axial machine. These efficiency errors are important to be considered, because

325

when the mean errors are averaged taken into account for all flow range, the obtained mean

326

error is lower than the absolute relative error near the BEP (e.g., when the radial machine is run

327

to 900 rpm, the absolute relative error is 0.06 and the mean square error is 0.02). Therefore, if

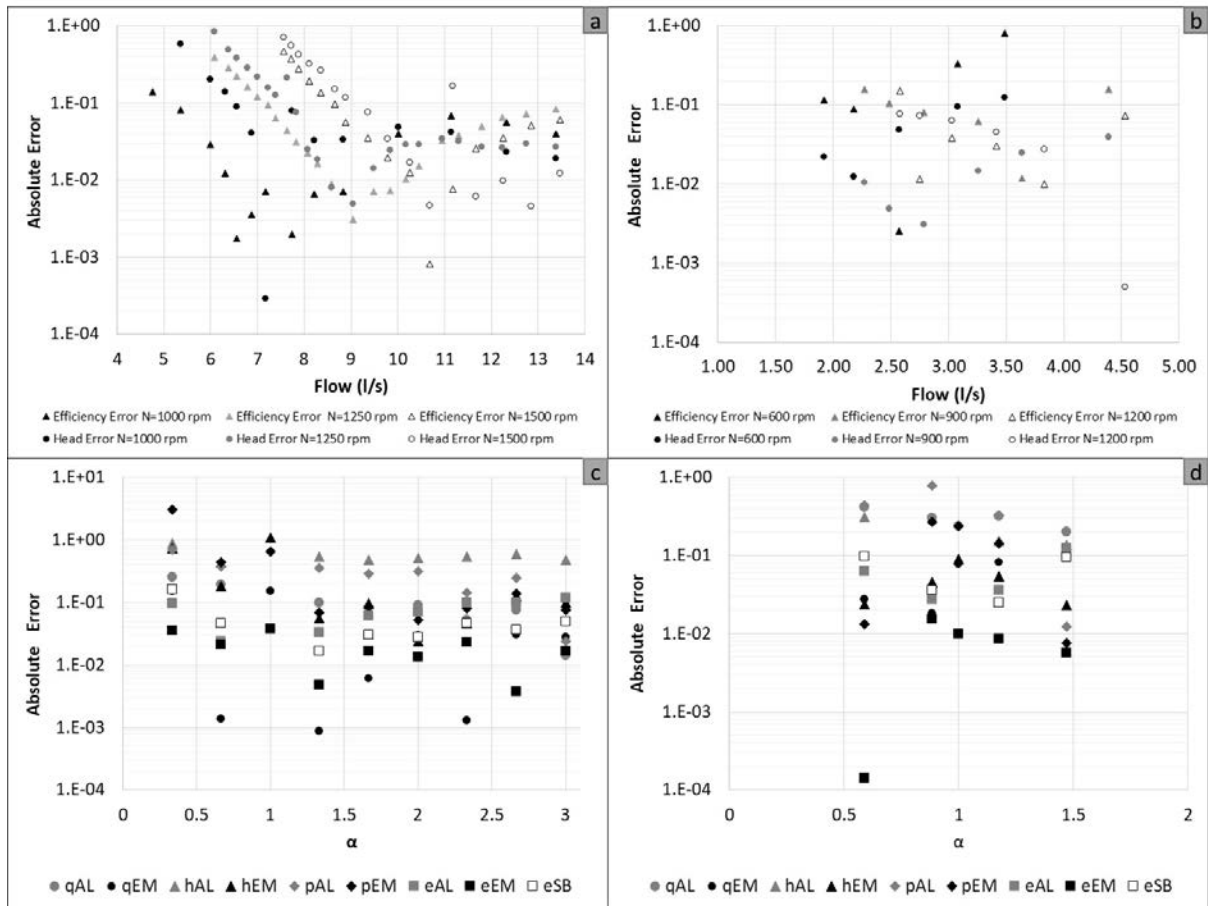
328

the mean error is determined for each speed, this can mislead to erroneous analyses. In the axial

329

machine, the mean square errors are 0.05, 0.04, and 0.06 for rotational speeds of 1000, 1250,

330 and 1500 rpm, respectively. These error values are not representative to analyze the maximum
 331 efficiency in the machine when the recovery system is operating by VOS. The mean square
 332 errors in radial machine are 0.09, 0.02, and 0.01 for speed of 600, 900, and 1200 rpm,
 333 respectively.



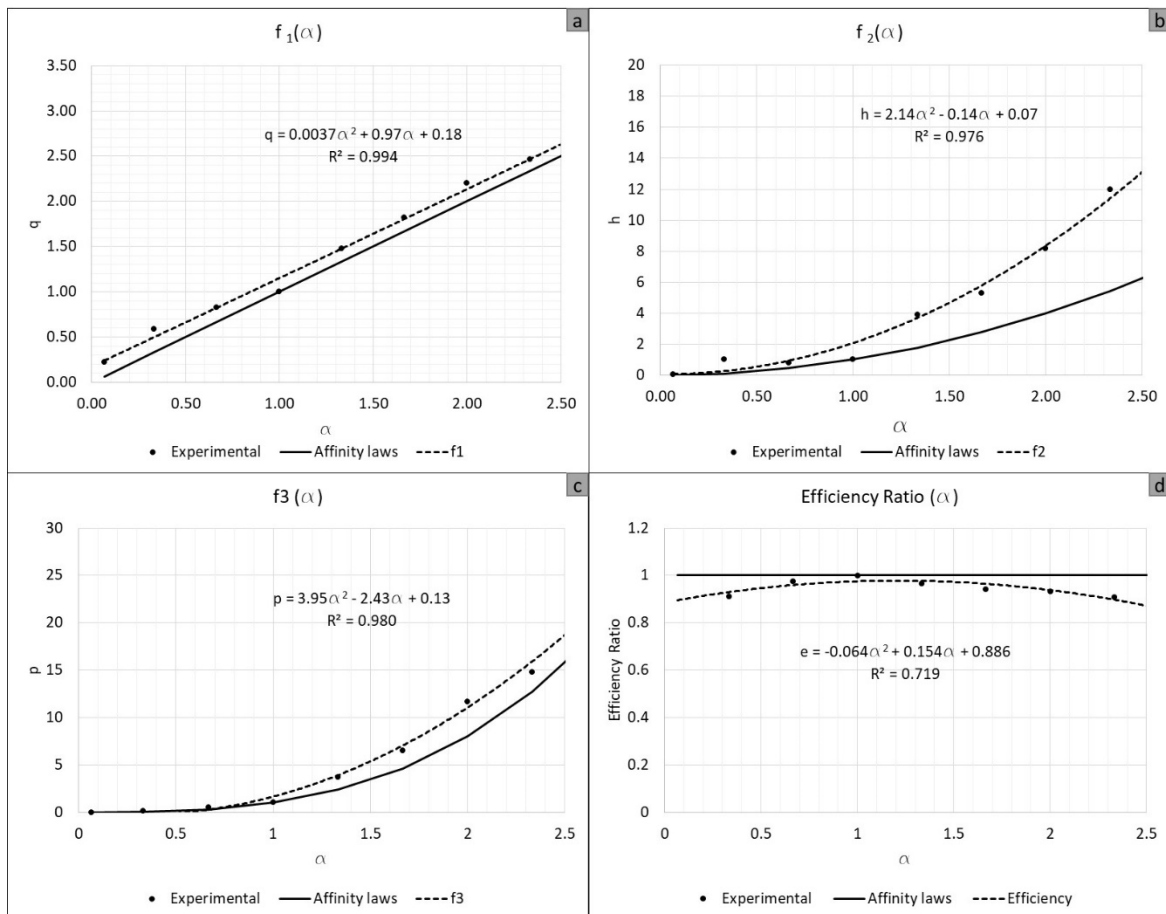
334
 335 **Fig. 4** Absolute error as a function of the flow and rotational speed in axial (a) and radial (b)
 336 machines considering the affinity laws. Absolute error in axial (c) and radial (d) machines
 337 when the parameters were determined by affinity laws (AL), empirical method (EM), and
 338 Sarbu-Borza method (SB)

339 3.4 Empirical method towards new affinity laws

340 If the shown errors in Figures 4a and 4b are taken into account, it is necessary to search for new
 341 solutions. These solutions have to allow modelers to determine functions with a less error, to

342 be used in the energy studies based on Suter Parameter (*SP*). To fit the affinity laws, the
 343 described methodology in section 2.3 enables to obtain such functions (f_1 , f_2 , and f_3). These
 344 functions lead for the determination of the *BEH* and the *BEL* in both machines, maximizing the
 345 efficiency in all ranges of flow by rotational speed variations.

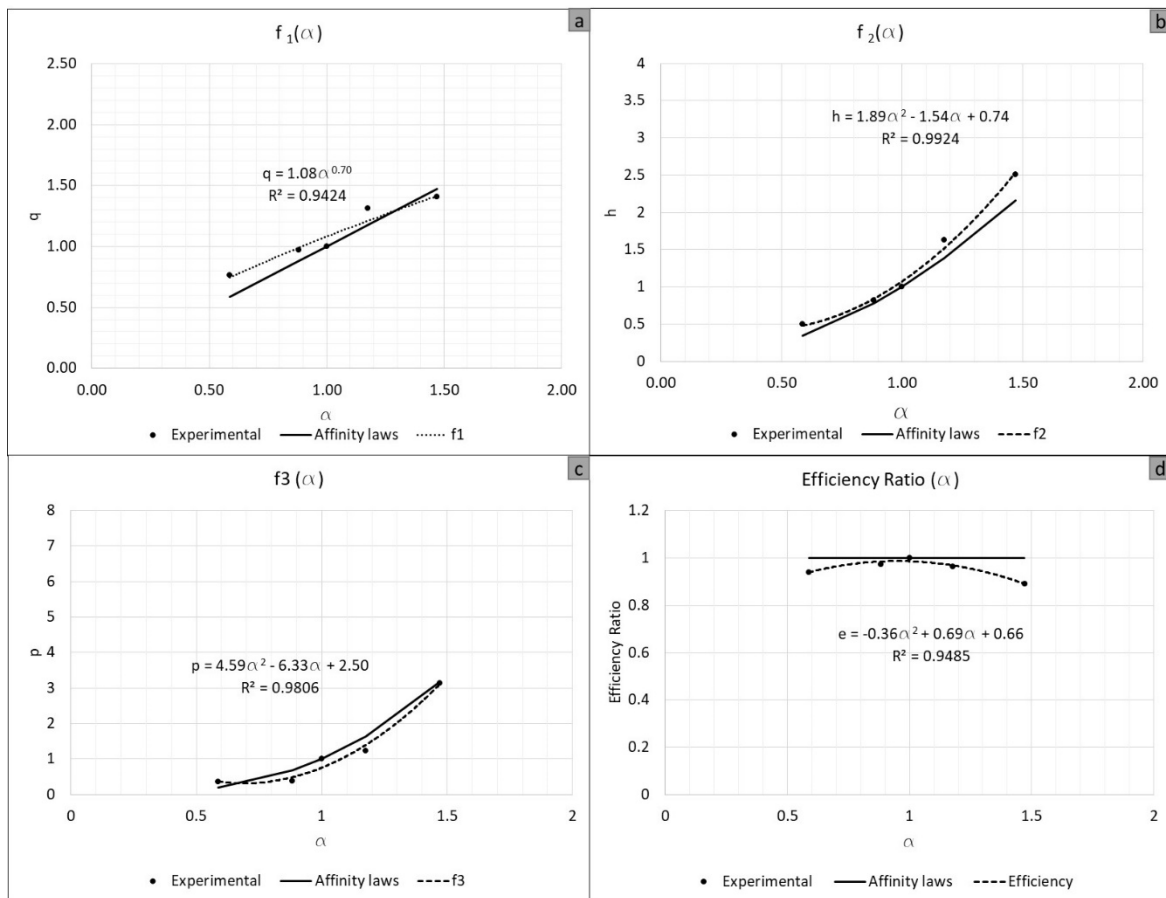
346 **Figures 5 and 6** show the proposed fitted functions for the axial and radial machines,
 347 respectively. To do a better analysis, other maximum values of efficiency were measured in the
 348 machine for rotational speeds of 250, 1750, 2000, and 2250 rpm. In the case of the radial
 349 machine, the maximum efficiency for the rotational speed of 1500 rpm has also been measured.
 350 In both machines, the obtained functions present good regression indexes that are higher to 0.94
 351 to parameters of q , h , p , and efficiency ratio, except the value of efficiency ratio in axial
 352 machine. For this machine, the value is 0.719.



353

Fig. 5 Proposed functions for axial machine.

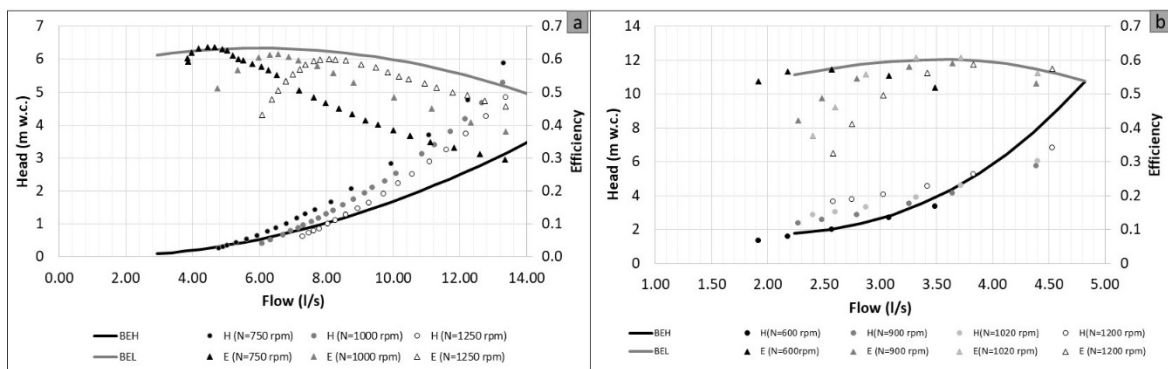
354 Once the functions for each parameter were adjusted by least squares, the errors can be
 355 calculated. The error results are shown in Figures 4c and 4d for both machines. The errors of q ,
 356 h , p , and efficiency ratio (e) are shown when the parameters are determined by affinity laws
 357 (AL), the proposed empirical method (EM), and Sarbu-Borza's Method (SB) (since this method
 358 is only used to determine efficiency values according to equation (13)). In all cases, the less
 359 error was obtained by EM. The obtained errors with SB were between the AL and EM. For the
 360 EM, the mean square errors were 0.02, 0.02, 0.004 for q , h , and efficiency ratio in the radial
 361 machine. When these values were determined for the axial machine, the errors were 0.02, 0.03,
 362 and 0.008, respectively. The mean square error by SB was 0.02 for both machines.



363

Fig. 6 Proposed functions for radial machine.

364 Once the errors were analyzed, the functions (f_1 , f_2 , and f_3) were known depending on the
 365 rotational speed. These functions enabled to draw the *BEL* and *BEH* of each machine. Figure 7
 366 shows these lines for the axial (Figure 7a) and the radial (Figure 7b) machines as function of
 367 flow, according to *VOS* described in Figure 1b. In the particular case of the radial machine, the
 368 *BEL* indicates that recovery system is working upper to 55% in the all range of flows. *BEL* and
 369 *BEH* are significant information in the optimization methodologies for water managers to
 370 develop the *VOS* in each hydraulic machine, thus maximizing the system efficiency.

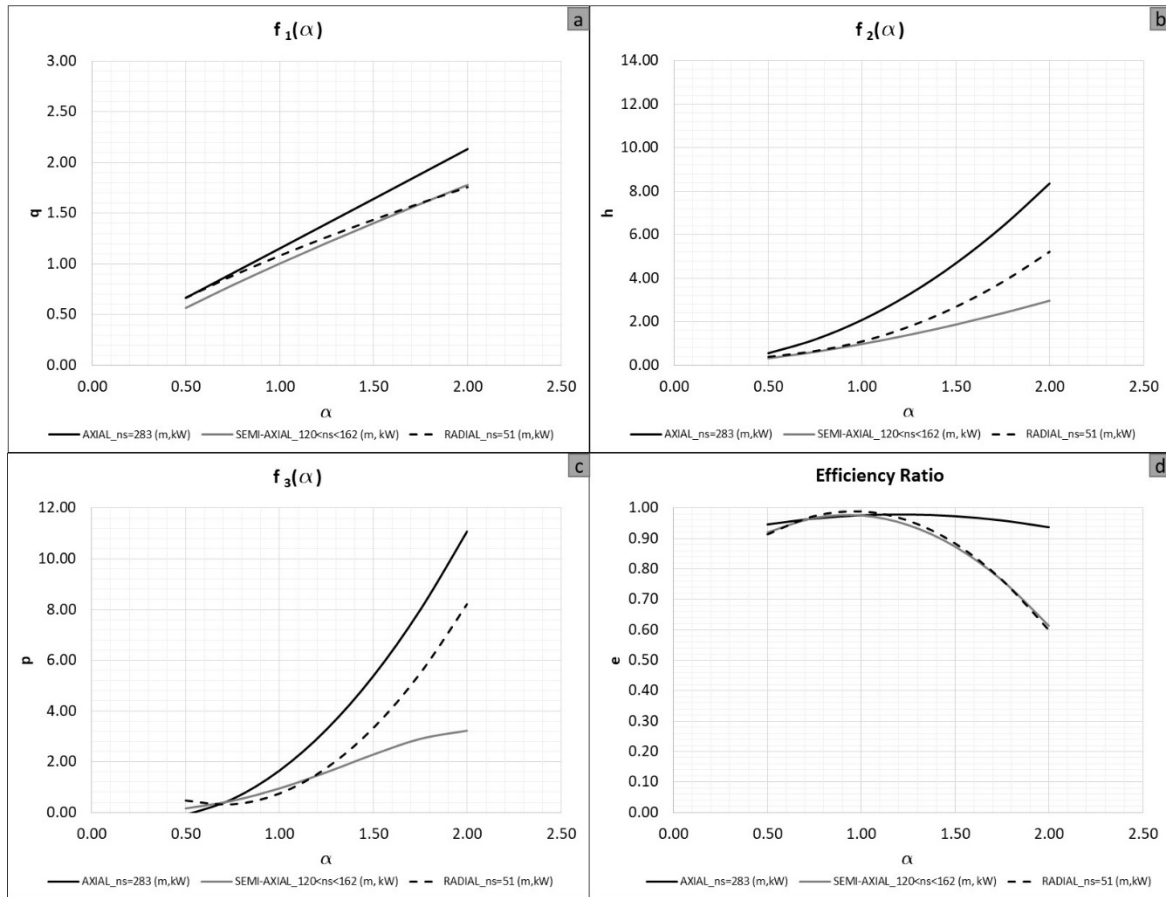


371

372

Fig. 7 *BEH* and *BEL* for axial (a) and radial (b) hydraulic machines

373 Finally, different functions as a function of the rotational speed can be drawn (*i.e.*, f_1 , f_2 , f_3 and
 374 e), joining the depicted procedure to modify the affinity laws with the analysis developed for
 375 semi-axial machines by Fecarotta et al. (2016). This analysis is shown in Figure 8 which
 376 correlates functions (*i.e.*, f_1 , f_2 , f_3 , and e) with the variables: velocity ratio and specific rotational
 377 speed.



378

379

Fig. 8 Fit function to different hydraulic machines.

380 These functions (f_1 , f_2 , f_3 , and e) presented relative and mean errors smaller than affinity laws
 381 and Sarbu-Borza's method when they were used to predict the real behavior of hydraulic
 382 turbines. When the radial machine was analyzed, the empirical mean square errors were 0.02,
 383 0.02, and 0.004 for q , h , and e parameters and the mean square error of affinity laws were 0.11,
 384 0.04, and 0.03, respectively. Therefore, the application of this empirical method reduced the
 385 mean error values in 81.81 %, 50%, and 86.67%, respectively. For the axial machine, the
 386 empirical mean errors were 0.02, 0.03, and 0.008, for q , h , and e parameters, respectively.
 387 Against, these errors were 0.06, 0.18, and 0.03 when the efficiency was determined by affinity
 388 laws, reducing them to 66.67%, 83.33%, and 73.33%, respectively.

389 4 CONCLUSIONS

390 This research presents experimental tests for two different hydraulic turbines (axial and radial)
391 that have a specific rotational speed of 283 and 51 (m, kW) respectively. For these machines,
392 the characteristic curves (flow-head, flow-mechanical power and flow-efficiency) were
393 obtained for different rotational speeds. The variable operating strategies (VOS) in recovery
394 systems of water distribution networks involve the need to predict the efficiency and head curve
395 of each machine for different rotational speeds. These curves will enable to develop viability
396 studies based on energy and economic analyses. These obtained curves are for a specific
397 reaction turbine and not general for all turbines.

398 The prediction of the efficiency with different rotational speeds by the classic affinity laws can
399 imply significant erroneous values. These errors induce the need to develop a modification in
400 the affinity laws to take into account losses in the impeller of each machine. In this research, as
401 novelty, new modified functions are proposed to know the flow, head, power and efficiency
402 parameters that depend on the rotational speed ratio for radial and axial machines.

403 These functions (f_1 , f_2 , f_3 , and e) were validated for the tested hydraulic machines, presenting
404 relative and mean errors smaller than affinity laws and the Sarbu-Borza's method. When the
405 radial machine was analyzed, the mean errors were reduced 81.81 %, 50%, and 86.67% for q ,
406 h , and e parameters when the errors were compared with the affinity laws. In contrast, the mean
407 errors were reduced 66.67%, 83.33%, and 73.33%, respectively for the axial machine.

408 The knowledge of these functions enables to develop the *BEL* and *BEH* lines as function of the
409 flow of each machine. These lines help managers to choose the best operating rules in order to
410 achieve the best efficiency point for each flow. These rules maximize the real recovered energy
411 under optimization strategies. Regarding the analysis of the rotational speeds, when the flows
412 are reduced, keeping a constant head the rotational speed increases in radial machine. This

413 phenomenon can cause that *PAT* reaches the runaway conditions when the machine is installed
414 in a line or point of a network **in which the flow variation is significant**.

415 Finally, the need to correlate the rotational speed and the specific speed with the different
416 characteristic parameters (*q*, *h*, *p*, and *e*) is of utmost importance. The development of similar
417 studies for different specific rotational speeds will **enable** to define the *BEL* and *BEH* **as well**
418 **as the selection** of the best hydraulic machine for each system characteristics.

419 **Acknowledgments**

420 This research is supported by Program to support the academic career of the faculty of the
421 Universitat Politècnica de Valencia 2015/2016 in the project “**Methodology** for Analysis of
422 Improvement of Energy Efficiency in Irrigation Pressurized Network”.

423 **Compliance with Ethical Standards**

424 **Conflict of Interest** The authors declare that they have no conflict of interest.

425

426 **REFERENCES**

427 Abbott M, Cohen B, (2009) Productivity and efficiency in the water industry. *Util. Policy*
428 17:233–244.

429 Alexander KV, Giddens EP, Fuller AM (2009) Radial- and mixed-flow turbines for low head
430 microhydro systems. *Renew Energy* 34:1885–1894. doi:10.1016/j.renene.2008.12.013

431 Araujo LS, Ramos HM, Coehlo ST (2006) Pressure Control for Leakage Minimisation in Water
432 Distribution Systems Management. *Water Resources Management* 20:133–149. doi:
433 10.1007/s11269-006-4635-3

434 Cabrera E, Cobacho R, Soriano J (2014) Towards an Energy Labelling of Pressurized Water
435 Networks. *Procedia Eng* 70: 209–217. doi:10.1016/j.proeng.2014.02.024

436 Carravetta A, Conte MC, Fecarotta O, Ramos HM (2014a) Evaluation of PAT performances
437 by modified affinity law. *Procedia Eng* 89:581–587. doi:10.1016/j.proeng.2014.11.481

438 Carravetta A, Del Giudice G, Fecarotta O, Ramos H (2013a) Pump as Turbine (PAT) Design
439 in Water Distribution Network by System Effectiveness. *Water* 5:1211–1225.
440 doi:10.3390/w5031211

441 Carravetta A, Del Giudice G, Fecarotta O, Ramos H (2012) Energy Production in Water
442 Distribution Networks: A PAT Design Strategy. *Water Resour Manag* 26:3947–3959.
443 doi:10.1007/s11269-012-0114-1

444 Carravetta A, Fecarotta O, Martino R, Antipodi L (2014b) PAT efficiency variation with design
445 parameters. *Procedia Eng* 70:285–291. doi:10.1016/j.proeng.2014.02.032

446 Corominas J (2010) Agua y Energía en el riego en la época de la sostenibilidad. *Ing del Agua*
447 17.

448 Dannier A, Del Pizzo A, Giugni M, Fontana N, Marini G, Proto D (2015) Efficiency evaluation
449 of a micro-generation system for energy recovery in water distribution networks. *Int. Conf.*
450 *Clean Electr Power* 689–694. doi:10.1109/ICCEP.2015.7177566

451 Derakhshan S, Nourbakhsh A (2008) Experimental study of characteristic curves of centrifugal
452 pumps working as turbines in different specific speeds. *Exp Therm Fluid Sci* 32:800–807.
453 doi:10.1016/j.expthermflusci.2007.10.004

454 Fecarotta O, Carravetta A, Ramos HM, Martino R (2016). An improved affinity model to
455 enhance variable operating strategy for pumps used as turbines. *J Hydraul Res* 1686:1–10.
456 doi:10.1080/00221686.2016.1141804

457 Fontana N, Giugni M, Portolano D (2012) Losses Reduction and Energy Production in Water-
458 Distribution Networks. *J Water Resour Plan Manag* 138:237–244.
459 doi:10.1061/(ASCE)WR.1943-5452.0000179

460 Giugni M, Fontana N, Ranucci A (2014) Optimal Location of PRVs and Turbines in Water
461 Distribution Systems. *J Water Resour Plan Manag* 140:06014004.
462 doi:10.1061/(ASCE)WR.1943-5452.0000418

463 Giustolisi O, Savic D, Kapelan Z (2008). Pressure-Driven Demand and Leakage Simulation for
464 Water Distribution Networks. *J Hydraul Eng* 134:626–635. doi:10.1061/(ASCE)0733-
465 9429(2008)134:5(626)

466 Gulich J (2003) Effect of Reynolds number and surface roughness on the efficiency of
467 centrifugal pump. *J Fluid Eng* 125:670–679.

468 Jiménez-Bello MA, Royuela A, Manzano J, Prats AG, Martínez-Alzamora F (2015)
469 Methodology to improve water and energy use by proper irrigation scheduling in pressurised
470 networks. *Agric Water Manag* 149:91–101. doi:10.1016/j.agwat.2014.10.026

471 Kevin B (1990) Optimization model for water distribution system design 115:1401–1418.

472 Mataix C (2009) *Turbomáquinas Hidráulicas*. Universidad Pontificia Comillas, Madrid.

473 McNabola A, Coughlan P, Corcoran L, Power C, Prysor Williams A, Harris I, Gallagher J,
474 Styles D (2014) Energy recovery in the water industry using micro-hydropower: an opportunity
475 to improve sustainability. *Water Policy* 16:168. doi:10.2166/wp.2013.164

476 Moreno M, Córcoles J, Tarjuelo J, Ortega J (2010) Energy efficiency of pressurised irrigation
477 networks managed on-demand and under a rotation schedule. *Biosyst Eng* 107:349–363.
478 doi:10.1016/j.biosystemseng.2010.09.009

479 Nazari A., Meisami H, (2008) Instructing WaterGEMS Software Usage. Tehran.

480 Pasten C, Santamarina JC (2012). Energy and quality of life. *Energy Policy* 49:468–476.
481 doi:10.1016/j.enpol.2012.06.051

482 Pérez-Sánchez M, Sánchez-Romero F, Ramos HM, López-Jiménez PA (2016) Modeling
483 Irrigation Networks for the Quantification of Potential Energy Recovering: A Case Study.
484 *Water* 8:1–26. doi:10.3390/w8060234

485 Pérez-Sánchez, M.; Sánchez-Romero, F.; Ramos, H.; López-Jiménez, P.A. (2017a). *Energy*
486 *Recovery in Existing Water Networks: Towards Greater Sustainability*. *Water*. 2017;9(2):97.

487 Pérez Sánchez, M.; Sánchez-Romero, F.J.; Ramos, H.; López-Jiménez, P.A. (2018). PATs
488 selection towards sustainability in irrigation networks: simulated annealing as a water
489 management tool. *Renewable Energy*, 116, 234-249.
490 <https://doi.org/10.1016/j.renene.2017.09.060>

491 Ramos HM, Borga A (1999). Pumps as turbines: an unconventional solution to energy
492 production. *Urban Water* 1:261–263. doi:10.1016/S1462-0758(00)00016-9

493 Ramos HM, Mello M, De PK (2010) Clean power in water supply systems as a sustainable
494 solution: from planning to practical implementation. *Water Sci Technol Water Supply* 10:39–
495 49. doi:10.2166/ws.2010.720

496 Ramos HM, Simão M, Borga A (2013) Experiments and CFD Analyses for a New Reaction
497 Microhydro Propeller with Five Blades. *J Energy Eng* 139:109–117.
498 doi:10.1061/(ASCE)EY.1943-7897.0000096

499 Rossman LA, 2000. EPANET 2: User’s manual, U.S. EPA. ed. Cincinnati.

500 Samora I, Franca M, Schleiss A, Ramos HM (2016a). Simulated Annealing in Optimization of
501 Energy Production in a Water Supply Network. *Water Resour Manag* 30:1533–1547.
502 doi:10.1007/s11269-016-1238-5

503 Samora I, Hasmatuchi V, Münch-Alligné C, Franca MJ, Schleiss AJ, Ramos HM (2016b).
504 Experimental characterization of a five blade tubular propeller turbine for pipe inline
505 installation. *Renew Energy* 95: 356–366. doi:10.1016/j.renene.2016.04.023

506 Sarbu I, Borza I (1998) Energetic optimization of water pumping in distribution systems. *Period*
507 *Polytech Ser Mech Eng* 42:141–152.

508 Shi G, Liu X, Yang J, Miao S, Li J (2015) Theoretical research of hydraulic turbine performance
509 based on slip factor within centripetal impeller. *Advances in Mechanical Engineering* 7(7):1–
510 12. doi:10.1177/1687814015593864

511 Simpson AR, Marchi A (2013). Evaluating the Approximation of the Affinity Laws and
512 Improving the Efficiency Estimate for Variable Speed Pumps. *J Hydraul Eng* 139:1314–1317.
513 doi:10.1061/(ASCE)HY.1943-7900.0000776

514 Singh P (2005) Optimization of the Internal Hydraulic and of System Design in Pumps as
515 Turbines with Field Implementation and Evaluation. University of Karlsruhe.

516 Suter P (1966) Representation of pump characteristics for calculation of water hammer. *Sulzer*
517 *Tech Rev* 66:45–48.

518 Ulanicki B, Kahler J, Coulbeck B (2008) Modeling the Efficiency and Power Characteristics
519 of a Pump Group. *J. Water Resour Plan Manag* 134:88–93. doi:10.1061/(ASCE)0733-
520 9496(2008)134:1(88)

521 Yang SS, Derakhshan S, Kong FY (2012) Theoretical, numerical and experimental prediction
522 of pump as turbine performance. *Renew Energy* 48:507–513.
523 doi:10.1016/j.renene.2012.06.002